Chirped Pulsed Four-Wave Mixing Spectrogram retrieval from from multiple shot-to-shot spectral measurement

Coralie Fourcade-Dutin, Frédéric Fauquet, Patrick Mounaix, Damien Bigourd

Chirped Pulsed Four-Wave Mixing Spectrogram retrieval from *from multiple shot-to-shot spectra*l measurement

Coralie Fourcade-Dutin, Frédéric Fauquet, Patrick Mounaix, Damien Bigourd*

***Abstract*— Four Wave Mixing generated from a chirped pump pulse in a photonic crystal fiber can provide large gain bandwidth and high gain value offering great parameters for ultra-short pulse amplification. However, the time to frequency distribution of the bands is an important feature to improve the maximum amplification performance. Here, we present a method to retrieve the spectrogram from multiple shot-to-shot spectral measurement using the dispersive Fourier transform method without the need to inject a seed and any iterative complex algorithm.**

***Index Terms*—Four wave mixing, Parametric amplifier, dispersive Fourier transform**

I. Introduction

Ultra-fast four wave mixing (FWM) is a promising process to parametrically amplify ultra-short pulses in an optical fiber at high gain with large bandwidth in a compact geometry [1-5]. As the process usually involves high power pulses, the pump and/or signal pulses are initially stretched before being injected in the fiber in order to avoid spurious nonlinearities or optical damage in the fiber. However, using a chirped pump pulse means that the instantaneous frequencies are temporally dispersed and the duration usually reaches few tens of ps or even ns. Therefore, the gain has temporal and spectral distributions which strongly depend on the fiber and pump properties according to the phased-matched FWM relation [6]. For an ultrashort pulse amplification, an ultrabroad band signal needs to be injected and the chirp signal should follow this time-frequency distribution to achieve the best gain bandwidth. Thus, it is very important to carefully characterized this time-frequency distribution to design a broadband FWM based amplifier.

This time-frequency distribution is often characterized from the amplitude and phase measurement with various well-known methods such as FROG [7], XFROG [8], GRENOUILLE [9], SPIDER [10]. These methods are usually dedicated to ultrashort pulse and involve optical interferometry, space to time coupling or delayed short gate to sample the pulse profile. Extended versions have also been implemented to include the space distribution [11, 12] or to measure long-chirped pulses [13,14]. In our specific case, the goal is to measure the time-frequency distribution of FWM based fluorescence, which is generated from a long-chirped pulse. As the fluorescence is an incoherent spontaneous emission from the interaction of the pump in the fiber, we focus on the time to frequency distribution without any phase retrieval using the Dispersive Fourier Transform (DFT) method.

DFT method has received considerable interest for its broad applicability and its simple implementation [15]. The broadband pulse under study propagates in a very long dispersive medium and each spectral component is delayed due to the group velocity dispersion. The long-chirped pulse is then detected with a fast photodiode and the temporal waveform fairly reproduces the spectrum in real time. We have recently shown that from statistical measurements of multiple shot-to-shot spectral measurements, the spectral correlation between the signal and idler photons reveals physical insights into the particular portion of the pump spectrum responsible for the FWM generation [16]. However, no spectrogram has been retrieved from the multiple shots. In this paper, we present a method to retrieve the spectrogram from the measurement of multiple shot-to-shot FWM spectra using the DFT method without injecting the signal with a simple and straightforward procedure. Compared to the previous work, we consider a long pulse with a duration of 500 ps at higher energy to ensure that the instantaneous frequencies within the bands are sufficiently delayed. In addition, as the pump spectrum lies in the normal dispersion regime of the photonic crystal fiber, the signal and idler lobes are significantly away from the pump. The full spectrum spans to more than 400 nm.

II. Principle

The general principle relies on the measurement of multiple shot-to-shot spectra of the FWM bands spontaneously generated from a long-chirped pulse. For each shot, two pump photons are converted to signal and idler photons, with different possibilities according to the phase matching criteria [17]. Once the shots are averaged, the FWM spectrum shape represents the gain profile of the parametric amplification in the unsaturated regime. From the statistical measurement over an ensemble of single shot FWM spectra, it is possible to evaluate the correlation between the signal and idler photons at a wavelength of λ_s and λ_i, respectively [16]. Instead, we can also identify the occurrence of each maximum in the Stokes and Anti-Stokes sides for each shot corresponding to a selected positive correlation. From the FWM photon energy conservation law (CL) i.e $2/\lambda_p=1/\lambda_s+1/\lambda_i$, it is straightforward to infer the origin of the FWM within the pump spectrum (with λ_p the pump wavelength). In our specific case, the pump pulse owns a high

This work was supported by the IdEx University of Bordeaux / Grand Research Program LIGHT. C. Fourcade-Dutin, F. Fauquet, P. Mounaix and D. Bigourd are with the IMS laboratory, UMR CNRS 5218, University of Bordeaux, 33405 Talence, France. (*damien.bigourd@u-bordeaux.fr*).

chirp leading to a long pulse duration in a range of few tens of ps. As the pump instantaneous frequencies are linearly spread in time, the pump pulse can be used as a temporal ruler once the instantaneous frequencies are identified. Thus, from the maximum occurrence, the time at which the idler and signal photons are generated can be retrieved to reconstruct a spectrogram leading to the time to frequency distribution.

We illustrate the principle of this method using numerical simulations by integrating the nonlinear Schrödinger equation with the split-step method. The used parameters were as follows. Firstly, the input pump pulse has a chirp of 83 ps/nm with a spectral bandwidth of 6 nm (at full width at half maximum-FWHM) centered at 1025 nm. This corresponds to a pulse duration of 500 ps (FWHM) as in the experiment. The pulse is injected in a 4-meter-long PCF which has a nonlinear coefficient of 11 $W^{-1}.km^{-1}$ and a zero-dispersion wavelength (ZDW) at 1028 nm. It means the pump spectrum lies in the normal dispersion regime. Initial noise is also included by adding one photon with a random phase on each spectral bin. In order to validate the performance of the DFT method, the PCF output is then injected in a 6.3 km long fiber (SMF28). The temporal profile is displayed in Figure 1.a and is compared to the shape of the spectrum obtained at the PCF output. The good agreement between the two shapes confirms the good behavior of the DFT part.

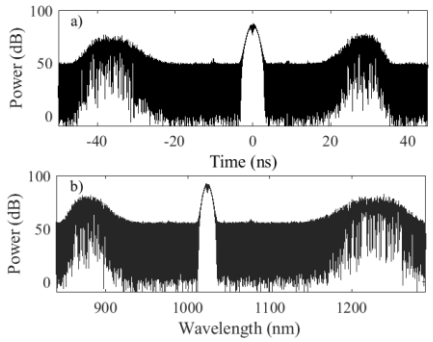

Figure 1. a) Waveform simulated at the output of the DFT. b) Simulated spectrum obtained after the PCF. The pump pulse duration is 500 ps.

As this simulation requires a large number of points (2^{25}) and a long temporal span (160 ns), we modified the simulation parameters to reduce the computation cost. The pump pulse duration is reduced to 50 ps due to a chirp of 8.3 ps/nm with the same peak power to reduce the number of points to 2^{15}. The pulse is then injected in the 5-meter-long PCF and 1000 simulations have been performed. Figure 2.a shows the ensemble of spectra (black line) and the average (red line) for an input peak power 250 W. Two FWM lobes are clearly observed at 900 and 1200 nm, similarly to the one obtained with a longer pulse duration. These two bands are numerically filtered (blue dashed lines) and then, the two spectrum maxima are selected for each single shot (Figure 2.b). This measurement represents the simultaneous occurrence of the signal and idler photons. For illustration, the blue arrows in Fig.2a corresponds to a particular example plotted in Fig. 2.b (blue cross). A well identified denser zone can be observed along a diagonal. As the two axes represent the wavelength of the signal and idler, the theoretical relationship of the FWM from the photon energy conservation law can be also plotted.

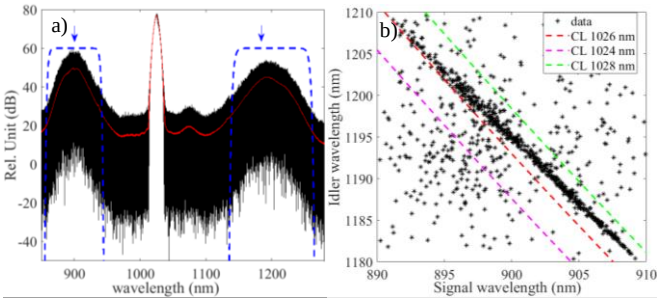

Figure 2. a) 1000 single shots (black line) and averaged spectrum (red line) of the simulated fluorescence spectra. b) Signal/Idler wavelength corresponding to the spectrum maxima of each FWM band. The lines are plotted from the photon energy conservation law for several pump wavelengths. The blue arrows in Fig.2.a corresponds to the particular case plotted in Fig. 2.b (blue cross)

The three lines displayed in Figure 2.b represent cases for a selection of wavelengths at 1024, 1026 and 1028 nm when a continuous wave pumps the PCF. Then, it is possible to infer the particular pump part, which generates the FWM bands. In our case with a chirped pulse with a large spectral bandwidth, the FWM bands are mostly generated from the pump part located between 1024 and 1028 nm. The known linear chirp of the pump is used to get the relative delay as the function of the pump instantaneous wavelength. For example, a null delay is set for 1025 nm and the shift of +/- 2 nm correspond to a relative delay of +/-16.6 ps. Therefore, from Figure 2.b and the pump chirp, the spectrogram shape of each FWM band be reconstructed (Fig. 2).

In order to validate the method, the correlation $\rho(\lambda_1, \lambda_1)$ between two wavelengths λ_1 and λ_2 within the two bands has been calculated from the ensemble of the single shot according to

$$\rho(\lambda_1,\lambda_2)=\frac{\langle I(\lambda_1)I(\lambda_2)\rangle-\langle I(\lambda_1)\rangle\langle I(\lambda_2)\rangle}{\sqrt{\langle I^2(\lambda_1)\rangle-\langle I(\lambda_1)\rangle^2\cdot\langle I^2(\lambda_2)\rangle-\langle I(\lambda_2)\rangle^2}} \quad (1)$$

where the angle brackets represent an ensemble average. The correlation varies from -1 to +1 indicating intensity fluctuations in the opposite or same directions respectively.

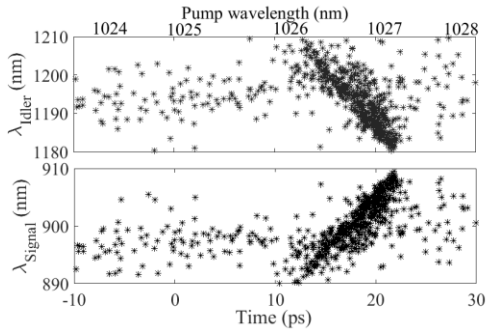

Figure 3. Retrieved spectrogram: bands maxima as the function of the time.

For ρ=0, no correlation exists between λ_1 and λ_2. In our case, the correlation maximum follows a λ_s-λ_i diagonal (Fig. 4.a) [16, 18] and similarly to the previous analysis, it is possible to conclude that the positively correlated bands are generated from the pump part with an instantaneous wavelength between 1024 and 1028 nm. The data corresponding to the maximum occurrences (as in Fig. 2.b) are also displayed and agree with the positive area of the correlation map. The spectrogram has

also been directly calculated from the electric field average with a 1 ps long gate (Fig. 4.b) to have the direct representation of the time-frequency distribution. The retrieved time-frequency distribution (white points) are in very good agreement with the directly calculated spectrogram confirming the great potentiality of the method; i.e the spectrogram can be effectively reconstructed from the multiple shot-to-shot spectral measurement.

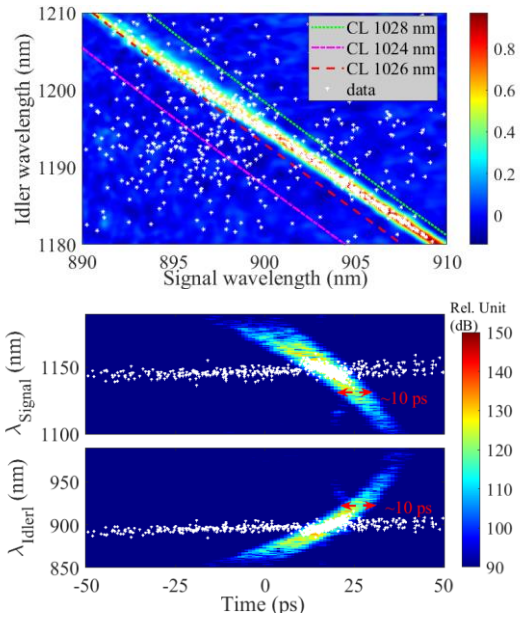

Figure 4. a) Correlation between the two bands calculated from the ensemble of single shot spectrum b) Spectrogram calculated from the electric field average with a 1 ps long gate. The white crosses correspond to the data obtained from the maximum occurrences as in Fig. 2.b and 3. **The red double-arrows provide an example of duration (10 ps) of a narrow spectral range.**

III. Experimental Implementation

The pump pulse is generated from an oscillator followed by a regenerative amplifier (S-pulse, Amplitude Systèmes) delivering a train of pulses at 85 kHz with a duration of ~300 fs and a spectrum centered at 1024 nm. The output beam is injected in a volume Bragg grating (VBG) that stretches the pulses to a duration of ~500 ps with a linear chirp. The pump pulse is then injected in a 5-meter-long PCF with similar properties of the ones used for the simulation. The injected peak power is 940 W. The average spectrum is firstly measured with an optical spectrum analyzer (OSA). Two FWM lobes are clearly observed and are located around 900 and 1220 nm (Fig. 5.a). At the PCF output, single shot spectra are also recorded by a dispersive Fourier transform set-up. It is composed of a 6.3 km long fiber (SMF28), a fast photodiode and an oscilloscope with a maximum bandwidth of 8 GHz. In this condition, the spectral resolution is estimated at ~1.1 nm. Figure 5.b shows a superposition of 1000 single shot spectra (black curves) and the averaged curve (red curve). To correctly map the spectrum into the time domain in the DFT technique, the far-field Fraunhofer dispersion condition must be satisfied [15]. This is usually obtained for a Fourier transform limited pulses stretched in a long dispersive fiber. Our configuration is considerably different since the FWM bands are spontaneously generated in the PCF and the spectral modes experience shot-to shot changes. In fact, the band durations are much shorter than the pump pulse duration. It can be seen on the spectrogram in Figure 4.b in which the spectral bands are temporally spread. For a narrow spectral range, the instantaneous pulse width is in the range of 10 ps (red double arrow in Fig. 4.b). The fidelity of the DFT part is validated since the spectrum recorded with the OSA is in good agreement with the scaled temporal waveform obtained after the DFT part (Fig. 5 a-b). This good agreement is a proof of the good behavior of the time-frequency mapping. The small discrepancy for the spectral position of the lobes is probably due to the high order dispersion term of the fiber. In addition, the SMF28 has been chosen for a cost-effective solution but it is lossy and not purely single mode in this full spectral range. Nevertheless, it has been proven that this fiber can provide a good representation even for this wide spectrum [19]. Similarly to the analysis of the simulated data, the two FWM bands are numerically filtered for all single shots. Then, the wavelength of the maxima on each side are recorded and plotted in Figure 6. The theoretical relationship of the FWM from the photon energy conservation law are also added for the 3 instantaneous pump wavelengths. It shows that the FWM maxima are generated from the center of the pump spectrum, mostly from 1024 nm. In addition, the signal and idler photons are uniformly spread and no clear dense zone are observed due to some experimental constraints. Along the propagation, the FWM bands are generated according to local dispersion profiles and also depends on the pump chirp. For example, in the case of a dispersion oscillating fiber, we demonstrate that the bands are not symmetric anymore compare to the case with a homogeneous dispersion. One band can be considerably narrowed while the other one becomes larger [20]. In addition, the input pump profile is another important key parameter since local temporal structures modify the peak power and therefore the FWM bands [21]. From the energy conservation, the scatter points can also be plotted as the function of the pump wavelength or the delay since the pump chirp is known from the VBG (Fig. 7). The signal is linearly spread in time while the full idler spectrum is generated at any delay. This information is very interesting and cannot be obtained from the average spectrum recorded with the OSA. It means the signal should be injected with a specific chirp of ~60 ps/nm, indicated by the red dotted line in Figure 7, for a broad band amplification. The correlation map between the two FWM bands have also been calculated for the ensemble of single shot spectra (Fig. 8). A positive value is observed with a specific shape with a maximum of ~0.6. The complete shape corresponds to the full FWM bands generated by the full pump bandwidth. As expected from the comparison between the numerical and experimental spectrogram, the correlation profile is different from the one obtained with the simulation. This discrepancy has already been observed with other analysis with a similar fiber [16]. The plotted CL lines (Fig. 8) highlight the position of the FWM generated by the middle part of the pump spectrum. The scatter data, obtained for the previously described analysis, follows the positive correlation part. This comparison also confirms that the method to retrieve the spectrogram is correct and useful to estimate the time-frequency distribution of the FWM bands pumped by a chirped pulse.

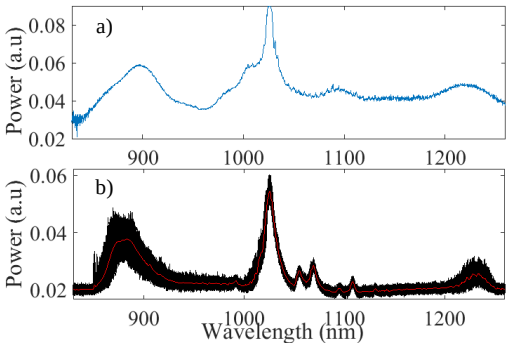

Figure 5. a) Fluorescence spectrum recorded with an OSA b) 1000 single shot spectra (black lines) recorded by the DFT and their average (red line)

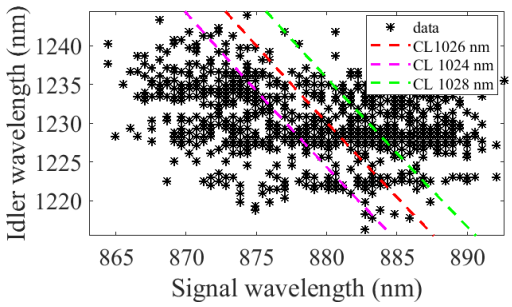

Figure 6. Signal/Idler wavelength corresponding to the spectrum maxima of each FWM band. The lines are plotted from CL for several pump wavelengths

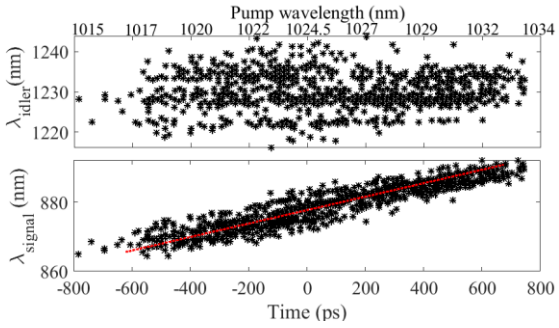

Figure 7. Retrieved spectrogram: maxima of the experimental bands as the function of the time.

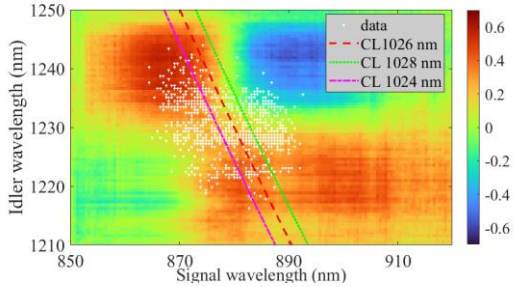

Figure 8. a) Correlation between the two bands calculated from the multi-shot spectrum. The white crosses correspond to the data obtained from the maximum occurrences. The lines are plotted from CL for several pump wavelengths.

IV. Conclusion

We have shown that the time-frequency distributions of the FWM bands can be retrieved from an ensemble of single shot spectra using the DFT method and the known pump chirp, without any complex algorithm. This technique is simple and straightforward to implement and leads to the spectrogram of the FWM bands. This retrieved profile is very important to set the best chirp of the signal seeding the photonic crystal fiber and to develop ultra-fast amplifier with a high gain-bandwidth.

REFERENCES

[1] D. Bigourd, L. Lago, A. Mussot, A. Kudlinski, J.F. Gleyze, E. Hugonnot, "High-gain, optical-parametric, chirped-pulse amplification of femtosecond pulses at 1 µm," Optics Letters **20**, 3480 (2010)
[2] L. Lafargue, F. Scol, O. Vanvincq, E. Poeydebat, G. Bouwmans E. Hugonnot, "All-polarization-maintaining and high energy fiber optical parametric chirped-pulse amplification system using a solid core photonic hybrid fiber," Optics Letters **47**, 4347 (2022)
[3] M. L. Buttolph, P. Sidorenko, C. B. Schaffer, F. Wise, "Femtosecond optical parametric chirped pulse amplification in birefringent step-index fiber," Optics Letters, **47**, 545 (2022)
[4] Y. Qin, O. Batjargal, B. Cromey, K. Kieu, "All-fiber high-power 1700 nm femtosecond laser based on optical parametric chirped pulse amplification," Optics Letters **28**, 2317 (2020)
[5] C Fourcade-Dutin, O Vanvincq, A Mussot, E Hugonnot, D Bigourd, "Ultra-broad band fiber optical parametric amplifier pumped by chirped pulses Part II: Sub-30 fs pulse amplification at high gain," Journal of Optical Society of America B **32**, 1488 (2015)
[6] D. Bigourd, P. Beaure d'Augères, J. Dubertrand, E. Hugonnot, A. Mussot, "Ultra-broadband fiber optical parametric amplifier pumped by chirped pulses," Optics Letters **39**, 3782 (2014)
[7] D.J. Kane, R. Trebino, "Characterization of arbitrary femtosecond pulses using frequency resolved optical gating," IEEE Journal of Quantum Electronics **29**, 571 (1993)
[8] A. M. Heidt, D.-M. Spangenberg, M. Brügmann, E.G. Rohwern and T. Feurer, "Improved retrieval of complex supercontinuum pulses from XFROG traces using a ptychographic algorithm," Optics Letters **41**, 4903 (2016)
[9] S. Akturk, M. Kimmel, P. O'Shea, R. Trebino "Measuring pulse-front tilt in ultrashort pulses using GRENOUILLE," Optics Express 11,491 (2003)
[10] L. Gallmann, D. H. Sutter, N. Matuschek, G. Steinmeyer, U. Keller, C. Iaconis, I. A. Walmsley, "Characterization of sub-6-fs optical pulses with spectral phase interferometry for direct electric-field reconstruction," Optics Letters **24**, 1314 (1999)
[11] T. Witting, F. Frank, C. A. Arrell, W. A. Okell, J. P. Marangos, J. W. G. Tisch, "Characterization of high-intensity sub-4-fs laser pulses using spatially encoded spectral shearing interferometry," Optics Letters **36**, 1680 (2011)
[12] D. Bigourd, J. Luce, E. Mazataud, E. Hugonnot, C. Rouyer, "Direct spectral phase measurement with Spectral Interferometry Resolved in Time Extra Dimensional." Review of Scientific Instruments **81**, 053105 (2010)
[13] A. S Wyatt, P. Oliveira, I. O. Musgrave, "Interferometric method for the complete characterization of highly chirped ultrabroadband pulses," arXiv 1612.08346v1 (2016)
[14] A. S Wyatt, P. Oliveira, I. O. Musgrave, "Frequency-resolved optical gating of highly chirped ultrabroadband pulses," arXiv:1612.05876v2 (2016)
[15] T. Godin et al. Advances in Physics : X **7**, 2067487 (2022)
[16] P. Robert, C. Fourcade-Dutin, R. Dauliat, R. Jamier, H. Muñoz-Marco, P. Pérez-Millán, H. Maillotte, J. Dudley, P. Roy, D. Bigourd "Spectral correlation of four-wave mixing generated in a photonic crystal fiber pumped by a chirped pulse," Optics Letters 45, 4148 (2020)
[17] D.R. Solli G. Herink, B. Jalali, C. Ropers "Fluctuations and correlations in modulation instability," Nature photonics **6**, 463 (2012)
[18] M. Touil, R. Becheker, T. Godin, A. Hideur, "spectral correlations in a fiber-optical parametric oscillator," Physical Review A **103**, 043503 (2021)
[19] Y. Qiu, C. Zhang, K.K.Y. Wong and K. Tsia "Dispersive Fourier transform using few-mode fibers for real-time and high-speed spectroscopy," In Proceeding of SPIE **8218**, 82180 (2012)
[20] C. Fourcade-Dutin and D. Bigourd, "Modulation instability in a dispersion oscillating fibre pumped by a broad band pulse," J. Mod. Optics **64**, 500 (2017)
[21] D. Bigourd, P. Morin, J. Dubertrand, C. Fourcade-Dutin, H. Maillotte, Y. Quiquempois, G. Bouwmans, E. Hugonnot, "Parametric gain shaping from a structured pump pulse," IEEE Phot. Technol. Lett. **31**, 214 (2019)